16th World Congress in Computational Mechanics (WCCM)
21-26 July 2024, Vancouver, Canada
A. Korobenko, M. Laforest, S. Prudhomme, R. Vaziri (Eds)

DYNAMIC MODELING OF TORSIONAL SEISMIC RESPONSE OF FRAME CORE-TUBE STRUCTURE AND CALIBRATION OF SUB-SYSTEM DESIGN PARAMETERS

Zhuang Guo[1], Zheng He[2,*], Xiao Lai[3]

[1] Graduate student, Department of Civil Engineering, Dalian University of Technology, Dalian 116024, China. E-mail: guozhuang@mail.dlut.edu.cn

[2] Corresponding author, Ph.D., Department of Civil Engineering, Dalian University of Technology, Dalian 116024, China. E-mail: hezheng@dlut.edu.cn

[3] Graduate student, Department of Civil Engineering, Dalian University of Technology, Dalian 116024, China. E-mail: Xiao_Lai_1994@mail.dlut.edu.cn

Key words: Frame Core-tube System, Torsional Ground Motion, Macroscopic Model, Parametric Calibration, NSGA-II Algorithm.

Abstract. To clarify the dynamic characteristics of the structure under torsional seismic excitation, a macroscopic dynamic model of the structure and simplified hysteretic models of each sub-system were established through theoretical derivation, and the accuracy of the models was verified using finite element models. To determine the design parameters of the hysteretic models for each sub-system, a multi-objective seismic optimization approach considering both structural cost and overall torsional damage was proposed. Through multi-objective optimization based on torsional overturning analysis, the design parameters of each sub-system were successfully determined. The results indicate that the outrigger truss sub-system plays a significant role in controlling the overall torsional behavior of the structure.

1 INTRODUCTION

Extensive earthquake damage indicates that torsional effects are one of the key factors leading to structural failure, especially for irregular structures. The frame core-tube structure is one of the most widely used structural systems in super-tall buildings [1]. With the diversified development of buildings, architects arrange the core tube eccentrically to form a frame core-tube structure with an eccentric inner tube to meet the functional and visual needs of the building. Under seismic or wind loads, the torsional effect of the structure is very significant. Through the efforts of scholars, some torsional control methods for such structures have been proposed [2]. In addition, regardless of whether the structure's plan is regular, the ground torsional component has a significant influence on the seismic response of the structure [3] Currently, there are few strong earthquake records of ground motion torsional components at home and abroad, and quantitative calculation parameters have not been provided. In the calculation of structural seismic effects, most only consider horizontal and vertical effects, and the torsional response of the structure obtained in this way tends to be unsafe. At the same time, the torsional failure mode of the structure will make it difficult for the multiple earthquake

defense lines set in the design process to function, leading to the difficulty in achieving the expected failure mechanism of the structure.

Currently, there is limited research on the torsional issues of super-tall frame core-tube structures, and various countries' codes only roughly control the torsion of structures through parameters such as torsional displacement ratio and relative eccentricity. There is a lack of in-depth research on the torsional issues of such structural systems. Establishing a macroscopic dynamic model of such structures under torsional ground motion excitation and simplified restoring force models of each subsystem is not only crucial for clarifying the torsional vibration mechanism of the structure but also significant for the design of model parameters for each subsystem. For each subsystem of the structure, the design parameters of the restoring force model are closely related to the component parameters, which involve many aspects such as component dimensions, section information, and material information. This complexity makes the calibration of design parameters extremely complicated. Therefore, due to the wide applicability of optimization algorithms in the field of structural design and their strong ability to solve complex problems, combined with some research results in the optimization field of reinforced concrete structures, it provides new ideas and tools from the perspective of structural optimization for the calibration of design parameters [4][5].

2 TORSIONAL SUBSYSTEM MODELING

2.1 Assumptions and simplifications

(1) The structural plan layout is symmetrical, and the floor heights remain constant vertically; the core tube wall does not deform in the plane, and the frame columns and core tube are fully fixed to the foundation; the model generally conforms to the assumptions of the torsional shear model calculation, and the development of plasticity at the end of the cantilever is considered using the assumption of concentrated plastic hinges.

(2) Only the effect of strengthened floors is considered, and the structure is divided into segments along the height of the strengthened floor area; the contribution of the hoop beams to the floor's torsional resistance is ignored; the floor mass is concentrated at the center of the floor slab, and only the vibration characteristics in the structural torsional direction are considered.

2.2 Torsional vibration equation

Research is conducted on the framework-core tube structural system as shown in Fig.1a. Based on the assumption conditions, the structural system is simplified to the structure shown in Fig.1b. To better describe the torsional mechanical behavior of the floor plan, the connection between the outrigger truss and the frame column is represented by equivalent spring and equivalent damping units, as shown in Fig.1d. We start by discussing a simple *N*-layer structure with *r* reinforced layers and rigid floors, where *r* is used to represent the number of reinforced layers in the structure. For the *r* mass sources in the structural system, according to the D'Alembert's principle of dynamic equilibrium, a dynamic system considering inertial forces is balanced at each instant. According to the isolator diagram of the *i*-th floor shown in Fig.1c, the forces on the isolator include external force T_i, restoring force $T_{S,i}$, damping force $T_{D,i}$, and inertial force $T_{I,i}$. The dynamic equilibrium for any mass source at a certain moment is:

$$T_{I,i}(t)+T_{S,i}(t)+T_{D,i}(t)=T_i(t) \tag{1}$$

Extend the dynamic equilibrium equation mentioned above to the entire structure, where each force vector is related to the structural torsional dynamic characteristic matrices **m**, **c**, **k**, and the input torsional excitation. Therefore, the simplified dynamic response of the structure under torsional excitation can be obtained by solving the following motion equation.

$$\mathbf{m}\ddot{\boldsymbol{\theta}}(t)+\mathbf{c}\dot{\boldsymbol{\theta}}(t)+\mathbf{k}\boldsymbol{\theta}(t)=\mathbf{-m1}\ddot{\boldsymbol{\theta}}_{\mathrm{g}}(t) \tag{2}$$

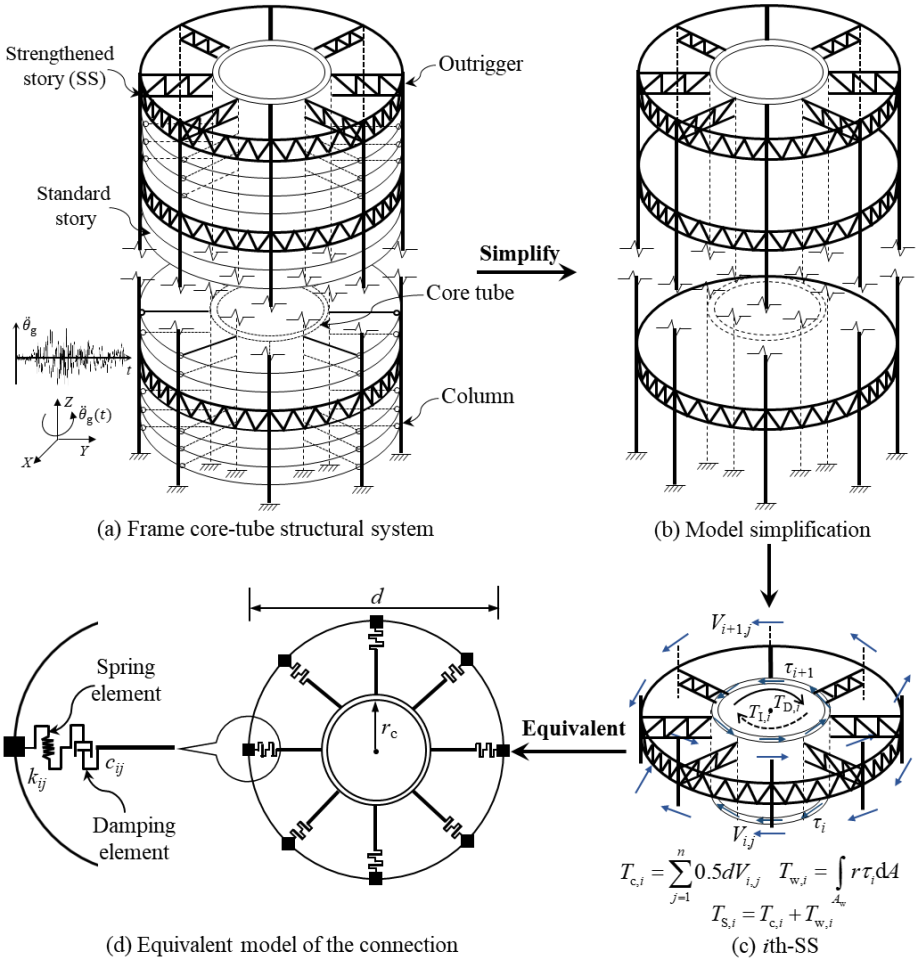

Figure 1: Establishment of torsional dynamics model

The torsional moment T_i acts at the center of the floor slab of the i-th floor of the structure. According to the force balance condition of the isolator, can obtain:

$$T_i = 4d(V_{\mathrm{c},i} - V_{\mathrm{c},i+1}) + T_{\mathrm{w},i} - T_{\mathrm{w},i+1} \tag{3}$$

For a column with a height of H, elastic modulus of E_{c}, and second moment of area of $I_{\mathrm{c},i}$, the lateral stiffness is given by $12E_{\mathrm{c}}I_{\mathrm{c},i}/H^3$. By introducing the lateral stiffness $k_{\mathrm{c},i}$ of the frame column, the shear force $V_{\mathrm{c},i}$ of the frame column is related to the inter-story shear deformation Δ_i. The inter-story torsional angle $\Delta\theta_i$ of the core tube can be calculated from the theory of torsional angle of thin-walled cylinders. The deformation coordination between the frame columns and the core tube in the floor plan is as follows.

$$\Delta_i = V_{\mathrm{c},i} / k_{\mathrm{c},i} \tag{4}$$

$$\Delta\theta_i = HT_{\mathrm{w},i} \Big/ 2\pi G r_{\mathrm{c}}^3 t_{\mathrm{w},i} \tag{5}$$

$$\Delta_i / (d/2) = \Delta\theta_i \tag{6}$$

Here, d and r_{c} represent the diameter of the floor slab and the radius of the core tube, G and $t_{\mathrm{w},i}$ are the shear modulus and the thickness of the shear wall of the core tube, respectively. By expressing $V_{\mathrm{c},i}$ and $T_{\mathrm{w},i}$ in terms of $\Delta\theta_i$ and substituting them into Eq. (3), and introducing the inter-story torsional stiffness $k_{\mathrm{t},i}$, the relationship between T_i and θ_i can be simplified as follows:

$$T_i = -k_{\mathrm{t},i}\theta_{i-1} + (k_{\mathrm{t},i} + k_{\mathrm{t},i+1})\theta_i - k_{\mathrm{t},i+1}\theta_{i+1} \tag{7}$$

$$k_{\mathrm{t},i} = 2d^2 k_{\mathrm{c},i} + 2\pi G r_{\mathrm{c}}^3 t_{\mathrm{w},i} \Big/ H \tag{8}$$

Expanding Eq. (8) to the entire structure, the stiffness matrix **k** can be established. For a linear elastic system, **k** holds true. However, under strong seismic action, when the deformation of the structure enters the elastoplastic stage, the elastic stiffness matrix is not suitable for solving the dynamic analysis of elastoplastic systems. The stiffness matrix **k** dynamically changes with the development of the structure's elastoplasticity.

The mass matrix is an r-order diagonal matrix with diagonal elements I_i. Throughout the entire motion process, the mass matrix is considered to remain unchanged [6]. I_i is contributed by the frame columns, outrigger trusses, and core tube in the floor plan, and can be calculated by the following equation:

$$I_i = \sum_{j=1}^{n_0} m_{ij} d_{ij}^2 \tag{9}$$

Here, n_0 represents the total number of components at the i-th level of the structure, and m_{ij} and d_{ij} respectively represent the translational mass of the j-th component at the i-th level and the horizontal distance between its center of mass and the center of the floor. Finally, the torsional mass matrix of the structure can be represented as $\mathbf{m}=\mathbf{diag}(I_1,\ldots,I_r)$.

Some researchers use Rayleigh damping to define the damping matrix of reinforced concrete structures when studying torsional response [7]. In calculating the Rayleigh damping coefficients, the damping ratios of each order of natural modes are taken as 5%, and the selected vibration modes are the first and third orders. The damping matrix is established as a linear combination of the mass matrix and the stiffness matrix.

$$\mathbf{c} = \mathbf{c}_{\mathbf{m}} + \mathbf{c}_{\mathbf{k}} = a_0\mathbf{m} + a_1\mathbf{k} \tag{10}$$

The simplified macroscopic dynamic model is verified through two aspects: torsional vibration period and floor torsional angle. The verification is conducted in both MATLAB and D-SAP programs to establish the macroscopic dynamic model and the simplified 4-story numerical model. Modal analysis is performed on the models, and the maximum errors for the first two torsional vibration periods are 5.36%. By applying torque to the structure and calculating the floor torsional angle using the SRSS combination method, the maximum error is 3.78%. Both error values are considered acceptable, indicating that the macroscopic dynamic model is reasonably accurate.

3 SUBSYSTEM HYSTERESIS MODEL

3.1 Frame column

The bilinear hysteresis model is widely used due to its simple form and effective description of complex nonlinear behavior in structures. Considering the advantages of the Q model [8] in

simulating nonlinear behavior of components and its suitability for this study, the Q model is selected to characterize the nonlinear behavior of components in each subsystem under seismic torsional excitation.

To determine the yield point design parameters of the frame column hysteresis model and establish the relationship between component cost and design parameters. The following assumptions are introduced: the column cross-section shape is square; the cross-section adopts a symmetrical reinforcement layout, neglecting the tensile effect of concrete; it is approximately assumed that the height of the equivalent rectangular compressive stress diagram is proportional to the section height h_i; stress analysis is based on the assumption of large eccentrically compressed members; the strains of concrete and reinforcement both follow linear variation; the beneficial effect of reinforcement on the section's bending stiffness is ignored. Under torsional seismic excitation, the frame column is in a composite state of bending moment and axial compression. The bending stiffness $E_cI_{c,i}$ of the column section at the i-th floor is given by the following equation. The concrete area $A_{c,i}$ of the column section can be approximated as the equivalent concrete area of the entire section.

$$k_{c,i} = E_c h_i^4 / 12 \tag{11}$$

$$A_{c,i} = h_i^2 = \left(12k_{c,i}/E_c\right)^{0.5} \tag{12}$$

The yield bending moment $M_{y,i}$ of the frame column can be determined by Eq. (13) where $A_{s,i}$ of the longitudinal tensile reinforcement in the section can be approximated by $k_{c,i}$ and $M_{y,i}$.

$$M_{y,i} = f_y A_{s,i} h_i + 0.5\left(1-\mu_i\right) N_i \tag{13}$$

$$A_{s,i} = \left[M_{y,i} \Big/ \left(12k_{c,i}/E_c\right)^{0.25} - 0.5\left(1-\mu_i\right) N_i \right] \Big/ f_y \tag{14}$$

where μ_i and N_i are the axial compression ratio and axial force of the i-th floor frame column, respectively, E_c is the elastic modulus of the cross-section concrete, f_y is the yield strength of the tensile reinforcement. In conclusion, the total cost C_0 of the frame column can be calculated by Eq. (15), in which n_c is the number of columns in the floor and C_c is the unit volume price of concrete and C_s is the unit weight price of steel.

$$C_0 = n_c r \left\{ C_c \sum_{i=1}^{r} \left(12k_{c,i}/E_c\right)^{0.5} + 7.85C_s \sum_{i=1}^{r} \left[M_{y,i} \Big/ \left(12k_{c,i}/E_c\right)^{0.25} - 0.5\left(1-\mu_i\right) N_i \right] \Big/ f_y \right\} \tag{15}$$

3.2 Outrigger truss

The rationality of spatial lattice steel outriggers is mainly reflected in their structurally optimized height. Several assumptions are introduced: the upper and lower chord rods are identical; the inertia moment of the chord rods is neglected; the outrigger height is equal to the floor height, with the width varying within a certain height-to-width ratio range; the entire section yields when the stress reaches the yield stress f_y; and the bending capacity of the vertical and diagonal rods is ignored. The outrigger is in a state of combined bending and shear stress, and the calculated schematic diagram is shown in Fig.2. By analyzing the outrigger, its bending stiffness $k_{b,i}$ and yield moment $M_{yb,i}$ around the y-axis can be obtained. Where $A_{bar,i}$ and $b_{b,i}$ are the chord area and width of the i-th floor outrigger truss, respectively, E_s is the elastic modulus of the tensile reinforcement. Then, introducing the total number of chord rods n_b and the length of the chord rods L in the strengthened layer, the total cost C_1 of the steel outrigger can be obtained.

$$k_{\mathrm{b},i} = E_{\mathrm{s}} A_{\mathrm{bar},i} b_{\mathrm{b},i}^2 \tag{16}$$

$$M_{\mathrm{yb},i} = 2 f_{\mathrm{y}} A_{\mathrm{bar},i} b_{\mathrm{b},i} \tag{17}$$

$$C_1 = 7.85 n_{\mathrm{b}} L C_{\mathrm{s}} \sum_{i=1}^{r} A_{\mathrm{bar},i} = 1.9625 n_{\mathrm{b}} L C_{\mathrm{s}} E_{\mathrm{s}} \sum_{i=1}^{r} \left(M_{\mathrm{yb},i}^2 / k_{\mathrm{b},i} \right) \Big/ f_{\mathrm{y}}^2 \tag{18}$$

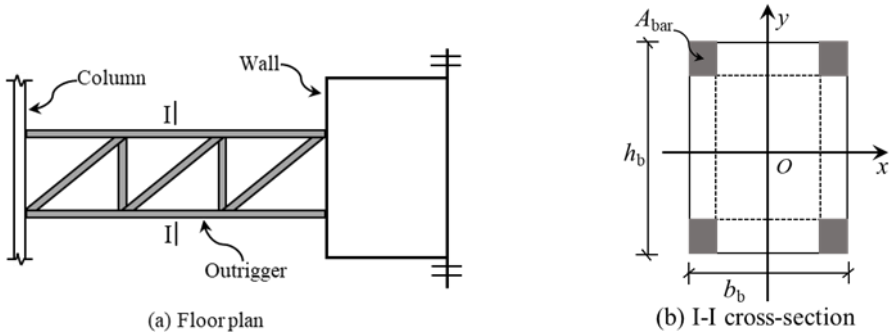

Figure 2: Simple calculation diagram of steel outrigger truss

3.3 Core tube

Several assumptions are introduced: the presence of openings in the core wall is ignored; stress is assumed to be uniformly distributed along the section's thickness direction; variations in longitudinal and horizontal reinforcement are neglected; and the core is considered a plain concrete structure where all moments and axial forces are borne by the concrete. The concrete core is subjected to the combined action of axial forces and torsion.The $\tau_{\max}$ is the maximum shear stress value in the annular section, σ_{y} is the axial compressive stress in the microelement, and τ_{xy} is the shear stress in the microelement. According to the theory of material mechanics, the torsional stiffness $k_{\mathrm{w},i}$ of the annular section of the core is $k_{\mathrm{w},i}=2\pi r_{\mathrm{c}}^3 G\delta_i$. The maximum principal tensile stress criterion is chosen as the yield condition for the section, expressed as a function $f(\sigma_{\mathrm{y}})$ of the normal stress, such that when τ_{xy} reaches the yield condition, the section is considered to have yielded to torsion, and the annular shear stress forms the yielding torsion moment $T_{\mathrm{y},i}$. By combining this with the formula for calculating the annular section area, the total cost C_2 of the core concrete can be obtained.

$$T_{\mathrm{y},i} = \int_A \tau_{\mathrm{xy}} r_{\mathrm{c}} \mathrm{d}A = 2\pi\delta_i r_{\mathrm{c}}^2 f(\sigma_{\mathrm{y}}) \tag{19}$$

$$C_2 = C_{\mathrm{c}} H \sum_{i=1}^{r} T_{\mathrm{y},i} \Big/ \left[r_{\mathrm{c}} f(\sigma_{\mathrm{y}}) \right] \tag{20}$$

4 NSGA-II-BASED PARAMETRIC CALIBRATION OF SUBSYSTEM

4.1 Problem formulation

Directly performing subsystem parameter design is quite difficult, so a multi-objective optimization strategy is adopted with the initial stiffness and yield strength of each subsystem as the optimization design variables. In reality, these optimization variables are related to the component's cross-sectional dimensions, material grades, and reinforcement ratios. To simplify the analysis, the material information of the components is not included in the optimization

scope. For frame columns and outrigger trusses, the initial stiffness and yield strength jointly affect the modeling parameters of the components and are included as optimization variables. For the core wall, the yield strength can be calculated from the initial stiffness, so only the initial stiffness is included as an optimization variable. In summary, the optimization design variables include the initial stiffness k_{col} and yield strength M_{col} of the frame columns, the initial stiffness k_{b} and yield strength M_{b} of the outrigger trusses, and the initial stiffness k_{w} of the core wall.

One of the most important objectives of structural optimization design is the cost of the design scheme. The cost of the structure consists of various aspects, mainly including material cost, labor cost, equipment cost, construction cost, etc. Here, in order to simplify the analysis, the focus is mainly on the variable-related cost changes in material cost. Structural torsional damage is chosen as another objective function. It conflicts with the structural cost objective because smaller structural damage usually implies higher cost, but it also indicates that the structure has higher energy dissipation capacity. Assuming that modal damage is mutually independent and in series, structural torsional damage is calculated using the structural damage calculation rules proposed by He and Guo [9].

Constraints in structural optimization under torsional excitation focus on overall stiffness, ductility, stability, uniform floor stiffness, and structural regularity. These constraints include limits on inter-story drift angles, column (or wall) axial compression ratios, stiffness-mass ratios, torsional stiffness ratios, and twist ratios. Converting floor plan rotations to inter-story drift angles for frame columns allows for the use of approximate limits for inter-story drift angles under lateral displacement. The stability of frame columns is crucial for overall structural stability, requiring stability analysis under lateral shear forces. Evaluating uniform floor stiffness distribution under torsional excitation involves introducing floor torsional stiffness ratios similar to lateral stiffness ratios, ensuring structural integrity and stability under torsional loading. From a civil engineering perspective, the optimization problem of structures under multi-objective seismic torsional excitation can be formulated using the above equation.

Find :

$$Find \quad \mathbf{X}=\left[k_{\mathrm{col},1},\cdots k_{\mathrm{col,r}},k_{\mathrm{b},1},\cdots k_{\mathrm{b,r}},k_{\mathrm{w},1},\cdots k_{\mathrm{w,r}},M_{\mathrm{col},1},\cdots M_{\mathrm{col,r}},M_{\mathrm{b},1},\cdots M_{\mathrm{b,r}}\right]^{\mathrm{T}} \tag{21}$$

To minimize :

$$f_1=C_0+C_1+C_2 \tag{22}$$

$$f_2=D \tag{23}$$

subject to :

$$s.t.\ g(\mathbf{X})=\begin{bmatrix} \max\left[(\theta_i-\theta_{i-1})/(2H/d)\right]_{\mathrm{FQ}}-0.00125 \\ \max\left[(\theta_i-\theta_{i-1})/(2H/d)\right]_{\mathrm{RQ}}-0.01 \\ N_{\mathrm{c}}/f_{\mathrm{c}}A_{\mathrm{c}}-0.75 \\ N_{\mathrm{w}}/f_{\mathrm{c}}A_{\mathrm{w}}-0.45 \\ 10-D(i)h(i)\Big/\sum_{i}^{n}G(i) \\ M_i\Delta\theta_{i+1}/M_{i+1}\Delta\theta_i-0.7 \\ 3M_i/\Delta\theta_i/\left(M_{i+1}/\Delta\theta_{i+1}+M_{i+2}/\Delta\theta_{i+2}+M_{i+3}/\Delta\theta_{i+3}\right)-0.8 \\ T_{\mathrm{t}}/T_1-0.85 \end{bmatrix}\le 0 \tag{24}$$

4.2 Twistover implementation and construction of optimization platform

Static nonlinear analysis avoids complex and time-consuming calculations while ensuring the stability of the results. Propose a toppling analysis method for torsional conditions based on the research background of this paper. The algorithm integration was performed on the self-developed finite element platform D-SAP [10], ultimately creating an executable program capable of recognizing and executing the torsional toppling analysis method.The NSGA-II optimization algorithm is based on the elitist strategy [11], inheriting the random characteristics of genetic algorithms while retaining the diversity of Pareto front solutions. Throughout the optimization process, NSGA-II plays a central role in controlling the overall framework. Its tasks include not only adjusting the parameters of the finite element model but also calling D-SAP for structural analysis and completing many operations related to the optimization algorithm. D-SAP primarily serves as a computational analysis tool, providing the response results required by the optimization algorithm. Due to its powerful interactive capabilities, MATLAB facilitates the implementation of the entire optimization process on this platform. The structural parameterized design process based on NSGA-II is shown in Fig.3.

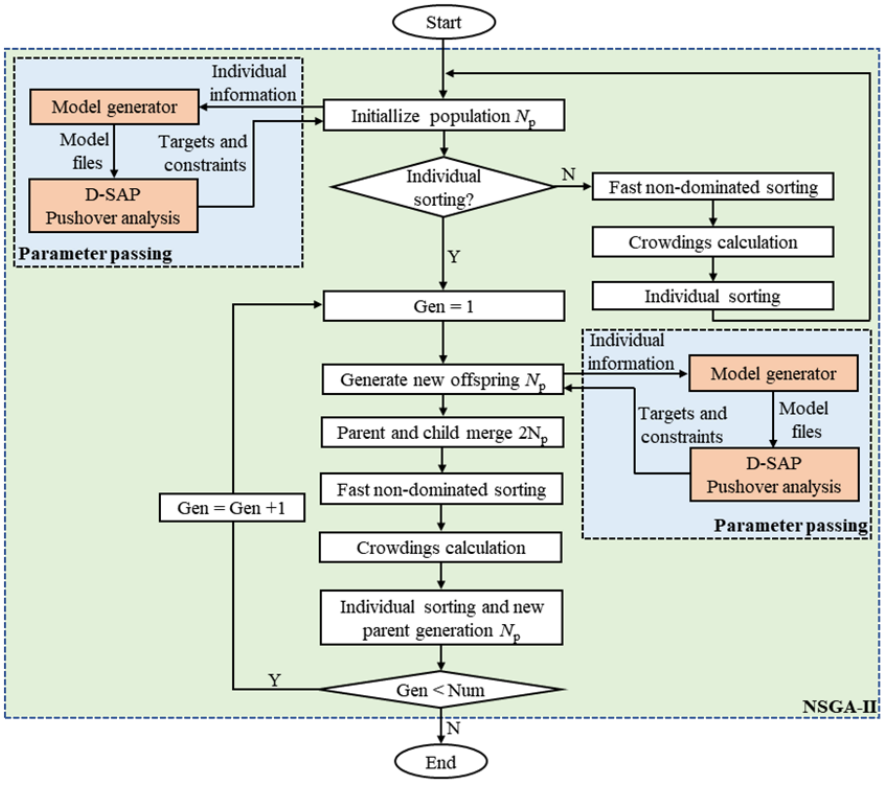

Figure 3: Optimization design process

5 CASE STUDY

5.1 Basic information

The case model is shown in Fig.4. According to the Chinese Seismic Design Code [12], the

seismic fortification intensity in the area is 7 degrees, with a site category of II and a design seismic grouping of the second group, with a site characteristic period of T_g=0.40s. The design floor live load and permanent load are 9kN/m² and 3kN/m² respectively. The material information for each component is shown in the figure. A 1% reinforcement ratio is assumed for ring beams and shear walls, while the amount of longitudinal reinforcement in frame columns varies dynamically.

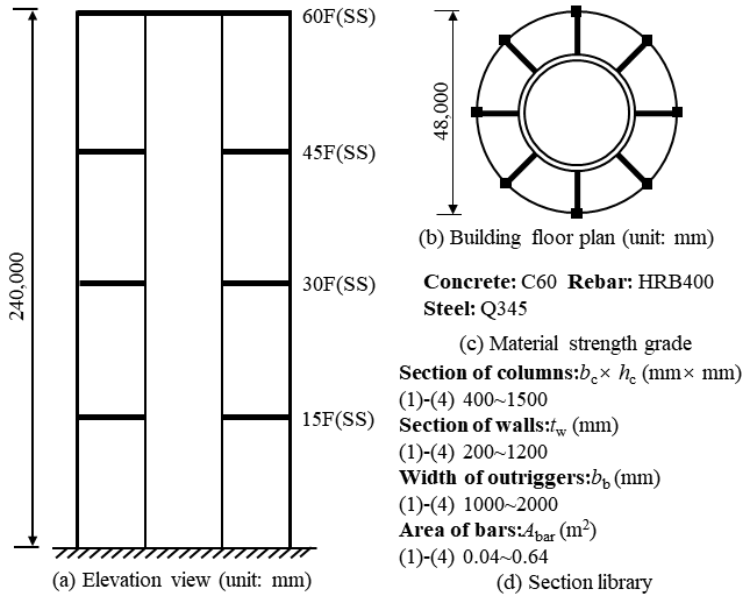

Figure 4: Frame core-tube case model

Establishing a finite element model in D-SAP, simulating circular beams and frame columns with displacement-based fiber beam and column elements, simulating core wall shear elements with layered shell elements, and simulating steel outrigger trusses with elastic beam elements. Each fiber element has four Gaussian integration points, using the Gauss-Legendre scheme. The concrete material is modeled using the Kent-Park model [13], and the steel reinforcement material is modeled using the Giuffre-Menegotto-Pinto model [14]. To consider the non-linear characteristics of the connection between the outriggers and frame columns, nonlinear zero-length elements are used. The structure is subjected to modal pushover analysis with twist angle displacement control loading. In the optimization process, the population size is set to 100, the number of iterations is set to 250, the crossover and mutation factors are set to 1.0 and 0.4 respectively, and the number of individuals selected in each tournament is set to 2. The optimization process was conducted on a workstation equipped with an Intel(R) Xeon(R) CPU Gold 6258R @ 2.7-4.0 GHz, taking approximately 60 hours for 250 iterations.

5.2 Results and discussion

Considering the inherent randomness of genetic algorithms, the optimization procedure was independently executed 5 times. Fig.5a demonstrates the acceptable stability of the improved NSGA-II. Fig.5b illustrates the distribution of all feasible solutions from the first optimization within the feasible domain. Three relatively unique feasible solutions were selected for design

parameter calibration: the optimal seismic performance individual from the Pareto solution set (Case A), the individual with the lowest structural cost (Case B), and an intermediate individual (Case C).

Fig.6 depicts the convergence history of the normalized objective $g_1(\mathbf{X})$ for Case A and Case B concerning the initial generation individuals. The optimization results exhibit a credible convergence trend, reflecting the inherent regulatory mechanism between objectives and complex constraints. Among these normalized constraints, the most significant maximum inter-story drift constraint tends toward 1. For both Case A and B, the axial compression ratio constraint of the frame columns gradually approaches 1 as the optimization progresses, while the axial compression ratio constraint of the shear walls in CaseA is more susceptible to optimization influences.

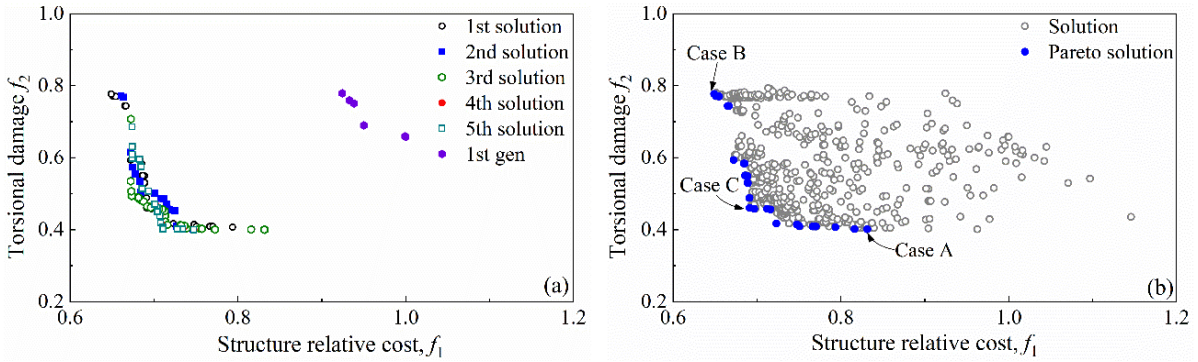

Figure 5: Optimization Results

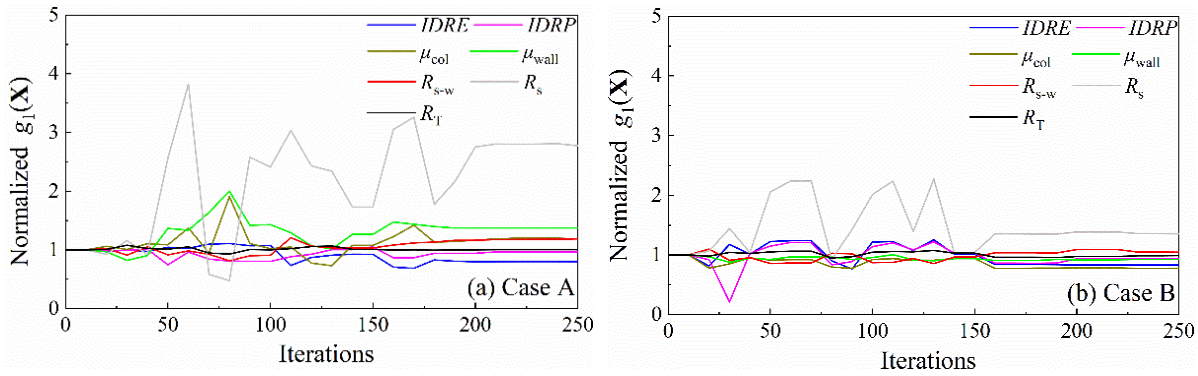

Figure 6: Convergence of normalized constraints during optimization process

Fig.7 shows the design parameter calibration results for the subsystem components of the frame columns, outrigger trusses, and core walls for the selected Cases A, B, and C. From the figure, it can be observed that there is little difference in the design parameters of the frame column subsystem components and the core wall subsystem components. However, the design parameters of the outrigger truss subsystem components for the high-performance Cases A are significantly larger than those for the other individuals. Additionally, it is noted that as the structure's cost decreases and the torsional damage increases from Case A to Case C and then to Case B, the design parameters of the outrigger truss subsystem exhibit a trend of gradually

decreasing. These observations indicate the significant influence of the outrigger trusses on the overall structural torsional resistance.

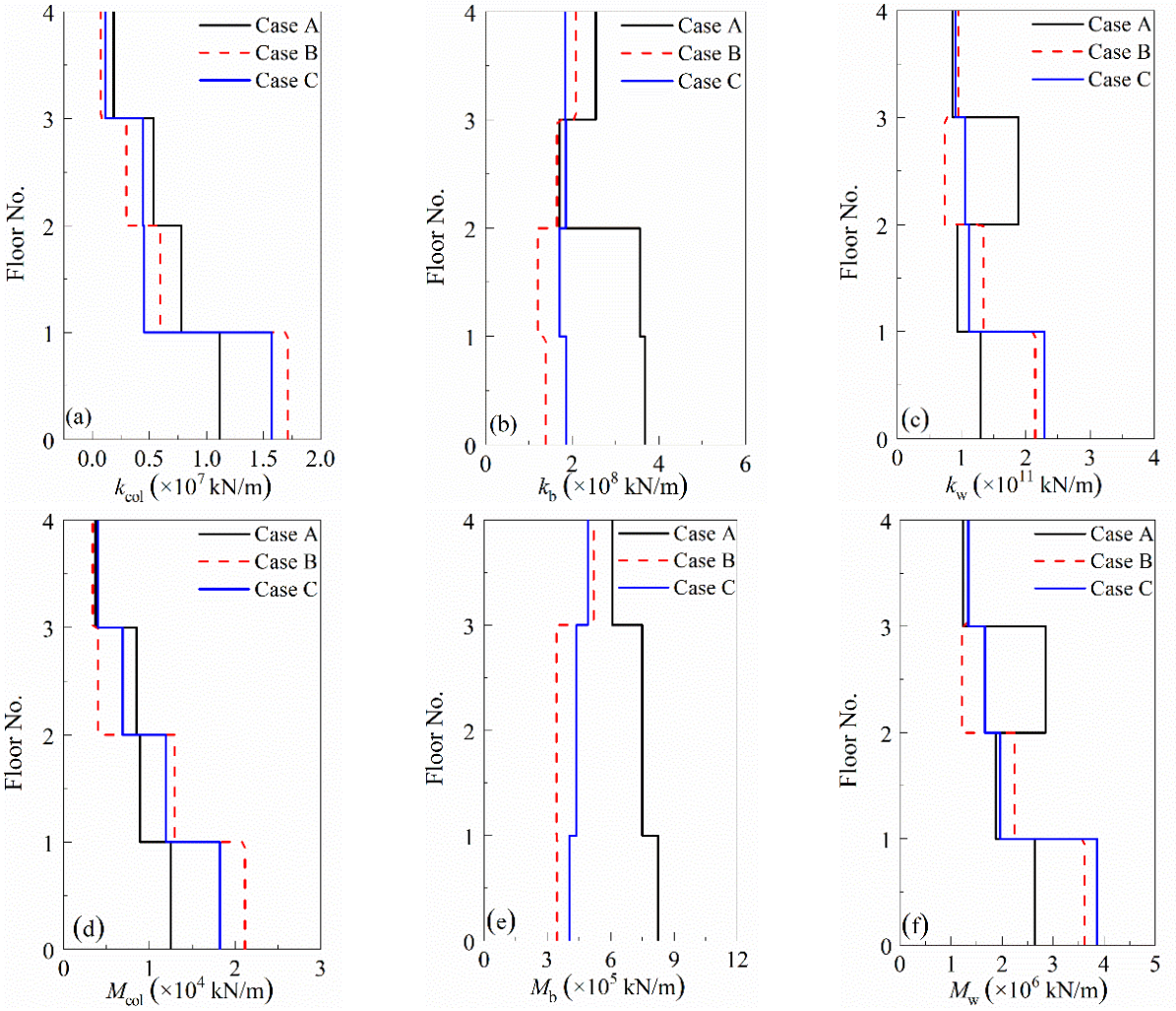

Figure 7: Distribution of individual design variables

6 CONCLUSION

The macroscopic model established in this paper can reasonably reflect the mechanical mechanism of the frame core-tube structure under torsional excitation, and the proposed torsional pushover analysis method has been implemented into the finite element program. Using a multi-objective genetic optimization algorithm that considers both torsional damage and structural cost, with the strength and stiffness of each subsystem component as optimization variables, as the calibration method, optimization is carried out on a simplified case structure using the established optimization implementation platform. Subsequently, the calibration of the design parameters of the selected representative individuals' hysteresis models is carried out, and the calibration results show that the outrigger truss subsystem has a significant impact on the overall torsional resistance of the structure.

7 ACKNOWLEDGEMENTS

The authors would like express their gratitude to the financial support from the National Natural Science Foundation of China (Grant No. 52078105).

REFERENCES

[1] Ding J, Wu H, Zhao X. Current situation and discussion of structural design for super high-rise buildings above 250 m in China [J]. Journal of Building Structures, 2014, 35(3): 1-7. (in Chinese).

[2] Ma Q. Study on torsional response control method of eccentricframe-core wall structures [J]. Structural Engineers, 2017, 33(5): 57-61. (in Chinese).

[3] Gupta V K, Trifunac M D. A note on contributions of ground torsion to seismic response of symmetric multistoried buildings [J]. Earthquake Eng. and Eng. Vibration, 1990, 10(3): 27-40.

[4] Du B, Li G, Wu Y, He Z, Qi Z, Huang G. Efficient storey lateral stiffness estimate and gradient-based multi-objective optimization of reinforced concrete frames with hybrid semi-rigid precast connections [J]. Eng Optim, 2021, 53(11): 1964–79.

[5] Tu X, He Z, Huang G. Performance-based multi-objective collaborative optimization of steel frames with fuse-oriented buckling-restrained braces [J]. Structural and Multi-disciplinary Optimization, 2020, 61(1): 365–79.

[6] Chopra AK. Dynamics of structures: theory and applications to earthquakeengineering [M]. University of California at Berkeley. 4th ed. Boston, USA: PearsonEducation Inc.; 2012.

[7] Dahmardeh S R, Motamedi M, Aziminejad A. Effect of torsional component of earthquakes on response of symmetric/asymmetric buildings [J]. Proceedings of the Institution of Civil Engineers-Structures and Buildings, 2020, 173(11): 858-878.

[8] M. Saiidi, M.A. Sozen, Simple and complex models for nonlinear seismic response of reinforced concrete structures [R]. Report No.: UILU-ENG-79-2013, Structural Research Series No. 465, University of Illinois, Urbana, IL, USA, 1979.

[9] He Z, Guo X, Zhang Y, Ou X. Global seismic damage model of RC structures based on structural modal properties [J]. J Struct Eng, 2018, 144(10).

[10] Fu S, He Z, Li Z, Tu X, Tao Q. Shared memory parallel computing procedures fornonlinear dynamic analysis of super high rise buildings [C]. In: Proc. the Secondnternational Conference on Performance-based and Life-cycle StructuralEngineering,Brisbane, Australia; 2015.p.1629-37.

[11] Deb K, Pratap A, Agarwal S, Meyarivan T. A fast and elitist multiobjective genetic algorithm: NSGA-II [J]. IEEE Trans Evol Comput, 2002, 6(2): 182–97.

[12] Ministry of Housing and Urban-Rural Development of People's Republic ofChina, 2016. Code for seismic design of buildings [S]. GB 50011-2016. China Architecture and Building Press, Beijing, China. (in Chinese).

[13] Scott B, Park R, Priestley M. Stress-strain behavior of concrete confined by overlapping hoops at low and high strain rates [J]. ACI Structural Journal, 1982, 79(1): 13-27.

[14] Filippou F C, Bertero V V, Popov E P. Effects of bond deterioration on hysteretic behavior of reinforced concrete joints [R]. Report No.: UCB.EERC-83/19, Berkeley,CA, USA: Earthquake Engineering Research Center, University of California at Berkeley, 1983.